



Cite this: DOI: 10.1039/c8nj05118f

# NHC stabilized Pd nanoclusters in the Mizoroki–Heck reaction within microemulsion: exploring the role of imidazolium salt in rate enhancement†

 Koena Ghosh,<sup>id</sup>\*<sup>a</sup> Shubhajit Dhara,<sup>a</sup> Sourav Jana,<sup>a</sup> Subhomoy Das<sup>id</sup><sup>b</sup> and Sudeshna Roy<sup>a</sup>

We report the significant rate enhancement of the Mizoroki–Heck reaction by *in situ* generated palladium nanoclusters within the confined space of water-in-oil (w/o) mixed microemulsion ( $\mu$ E) formulated by sodium dodecylsulfate (SDS), polyoxyethylene (23) lauryl ether (Brij-35) and isopropyl myristate (IPM), in the presence of novel imidazo[1,5- $\alpha$ ]pyridinium chlorides as N-heterocyclic carbene (NHC) precursors. This is the first endeavor to study an organic reaction in microemulsions containing IPM as a biocompatible green oil. A series of novel imidazo[1,5- $\alpha$ ]pyridinium chlorides were synthesized in a cost effective manner and were screened for a typical Heck reaction between 4-iodotoluene and <sup>n</sup>butylacrylate. The optimum rate was achieved with 2-hydroxyphenylimidazo[1,5- $\alpha$ ]pyridinium chloride at low catalyst loading under mild conditions. Conductivity and FTIR measurements suggested an effective change in the hydrogen bonding network of interfacial water in the presence of the NHC-precursor. Strong evidence for *in situ* formation of the Pd–NHC complex was obtained which significantly accounts for the rate enhancement. The reaction progresses rapidly with non-activated and sterically hindered aryl halides under optimal conditions. We further report a unique isolation technique to separate IPM (oil) from the reaction medium. The effect of NHC-precursors within the confined space of a microemulsion, wherein the reaction takes place, is correlated with the observed rate enhancement.

 Received 8th October 2018,  
Accepted 20th December 2018

DOI: 10.1039/c8nj05118f

rsc.li/njc

## Introduction

Metal-catalyzed organic transformations have been recognized as useful synthetic techniques to construct C–C bonds leading to the formation of various complex molecular scaffolds having significant pharmaceutical and material properties. These transformations rely on two crucial factors: a specific ligand for activating the metal center and the nature of the reaction medium. Over the past few decades, remarkable progress in the design of N-heterocyclic carbene (NHC) based ligands has been accomplished by taking advantage of their strong  $\sigma$ -donor capacity, thermal stability and low dissociation rates with tunable electronic and steric properties.<sup>1</sup> The higher stability of metal–NHC (M–NHC) species enabling them to participate in reactions under diverse conditions adds to their potentiality for widespread application in homogeneous catalysis,<sup>2</sup> *e.g.* cross-coupling reactions, C–H activation, metathesis, *etc.*, for the

preparation of pharmaceuticals<sup>3</sup> and advanced materials.<sup>4</sup> A recent report shows an alternate cocktail-type catalysis in the Pd–NHC catalyzed Mizoroki–Heck reaction where cleavage of a metal–NHC bond plays a crucial role in catalysis.<sup>5</sup> Driven by the recent challenges in sustainable chemistry,<sup>6a,b</sup> development of novel reaction media containing water to achieve a higher rate, ambient reaction temperature, low catalyst consumption, easy product separation and catalyst recovery is particularly advantageous.<sup>6</sup> However, the insolubility of organic compounds in water tends to limit its applicability in a broad sense. A number of existing unconventional solvents employing imidazole based ionic liquids,<sup>7</sup> ionic organic bases,<sup>8</sup> inexpensive amphiphiles forming micelle or reverse micelle,<sup>7c,9–11</sup> *etc.*, are known to address insolubility issues associated with water.<sup>11</sup> These entities are able to co-solubilize inorganic salts, as well as otherwise insoluble organic compounds in water.

Notably, water-in-oil (w/o) microemulsion systems are homogeneous mixtures of oil, water, surfactant and/or co-surfactant, which contain individual domains of oil and water separated by a monolayer of surfactant and/or co-surfactant at the microscopic level. The highly dynamic charged interfacial region of these microstructures allows easy accumulation of reacting species at the monolayer where water soluble components get

<sup>a</sup> Department of Chemistry, Presidency University, 86/1 College Street, Kolkata 700 073, India. E-mail: koena.chem@presiuniv.ac.in; Fax: +91-33-2241-3893; Tel: +91-33-2241-3893

<sup>b</sup> Department of Chemistry, Indian Institute of Technology Kanpur, Kanpur-208016, India

† Electronic supplementary information (ESI) available. See DOI: 10.1039/c8nj05118f

encapsulated into the water domain.<sup>12</sup> Such droplet based nano-sized micro-fluids serve as nano-reactors which break down and recombine within nanosecond time scale and allow very fast material exchange. This facilitates a reaction resulting in optimum reagent consumption and rapid mixing of substrates in terms of improved reaction rates.<sup>11,13</sup> Water in nanodroplets exhibits properties different from bulk due to imposed geometric constraints from the restrictive H-bonding network. This unique physicochemical behaviour of microemulsions gives rise to exceptional chemical reactivity when used as a solvent.<sup>11</sup> Moreover, such systems have already been recognized as economically viable templates for the preparation of nanoparticles in a simple manner.<sup>7,14</sup> A crucial balance between stability and flexibility of the microemulsion is essential to achieve optimum rate enhancement which relies on the system composition, temperature, and nature of the additive used.<sup>15</sup>

The present study usefully combines the advantages of a w/o microemulsion system as reaction medium with heightened reactivity of *in situ* generated NHC–Pd catalyst in the Mizoroki–Heck coupling reaction at ambient condition as a benchmark for evaluation. We have prepared novel NHC-precursors for this purpose. This extremely useful catalytic reaction often requires temperature higher than or in the vicinity of 100 °C, even in water or in a microemulsion.<sup>7c,16,17</sup> We are able to conduct successful coupling reactions in isopropyl myristate (IPM) blended biocompatible microemulsion, typically around 45 °C *via* an operationally simple protocol. We report herein the experimental results of the remarkable rate enhancement of the Mizoroki–Heck reaction under optimized conditions. Our systematic investigation illustrates how perturbation induced by the NHC-precursor encapsulated confined space of an organized assembly affects the rate of the reaction within ‘nano-reactor’, by conductivity and vibrational spectroscopic measurement *via* D<sub>2</sub>O probing. Recently, imidazolium-based surface-active ionic liquids were reported to promote the Suzuki reaction in microemulsion at room temperature using conventional organic solvent.<sup>7b</sup> In contrast, we have carefully chosen IPM based biocompatible  $\mu$ E as a green reaction medium. We have developed a unique isolation technique to separate IPM (oil) from the reaction medium. The recyclability of the catalytic system is also discussed. To the best of our knowledge, such a comprehensive study on IPM-derived w/o mixed surfactant microemulsion as a biocompatible template for catalytic organic transformation has not been reported in the literature so far.

## Results and discussion

We prepared three types of water-in-oil (w/o) microemulsion systems with single anionic (sodium dodecylsulfate, SDS), non-ionic (polyoxyethylene (23) lauryl ether, Brij-35) and equimolar mixture of anionic–nonionic (SDS/Brij-35) surfactants using isopropyl myristate (IPM) as the bulk oil phase. Surfactants (SDS and Brij-35) having same hydrocarbon chain length (constituting 12 carbon atoms in the linear chain of the tail) were typically chosen to minimize possible interactions between the

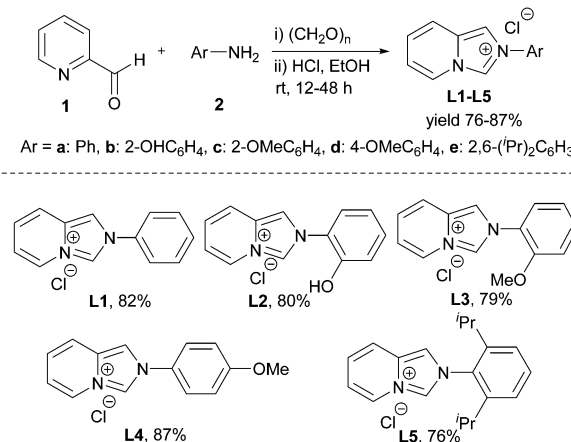
hydrocarbon tails of the two surfactants.<sup>18a</sup> The choice of IPM was made considering its biocompatible nature and extensive use in drug delivery systems.<sup>18b,c</sup> In addition, 1-pentanol was used as the co-surfactant (Pn) for stabilization of the system due to its biological and technological implications.<sup>19</sup> Notably, mixed surfactants play a prominent role in surface chemical applications because they are cost effective and often exhibit pronounced interfacial properties. The interactions between the constituent surfactants can lead to either synergism (attractive) or antagonism (repulsive) based on their physicochemical properties. At the equimolar composition of ionic–nonionic mixed surfactant, superior activity is commonly achieved compared to the individual components.<sup>20</sup>

### Synthesis of imidazo[1,5- $\alpha$ ]pyridinium ions from pyridine-2-carboxaldehyde

A few novel imidazo[1,5- $\alpha$ ]pyridinium chlorides with varying degrees of steric and electronic properties were prepared from commercially available pyridine-2-aldehyde, aryl amines and formaldehyde in the presence of a catalytic amount of HCl following a single step protocol (Scheme 1).<sup>21</sup> The pure salts were obtained in 76–87% yields after crystallization from acetonitrile/THF or ethanol/diethyl ether. Characterization of all the new compounds was done by spectroscopic studies.<sup>22</sup>

### Encapsulation of the NHC-precursor in the chosen microemulsion droplet

The imidazolium salts (**L1–L5**) were encapsulated in chosen anionic, non-ionic and mixed w/o microemulsion templates (0.02 mmol in  $\sim$ 2 mL) at  $\omega$  20, in which NHC-precursors containing aqueous nanodroplets were suspended in the bulk oil phase stabilized *via* the surfactant monolayer.<sup>22,23</sup> The NHC-precursors in such a system are likely to orient at the oil–water interface in such a way that the polar part of the molecule enters the water domain and the non-polar part extends into the hydrocarbon tail of the surfactant molecules (or surfactant palisade layer). The formation of optically isotropic, transparent and stable homogeneous dispersions of NHC encapsulated w/o microemulsion was also evident from visual observation (Fig. 1).



Scheme 1 Preparation of imidazo[1,5- $\alpha$ ]pyridinium chloride, **L1–L5**.

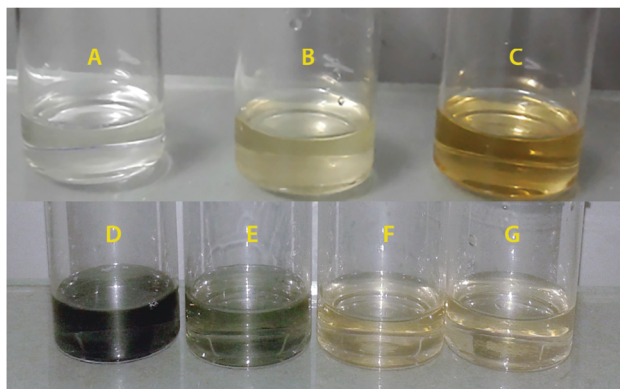


**Fig. 1** Representative photographs of water-in-oil (w/o) single and mixed microemulsion (SDS/Brij-35/Pn/IPM,  $\omega = 20$ ) in the absence and presence of an active NHC-precursor. (A) Mixed  $\mu$ E, (B) mixed  $\mu$ E containing **L1**, (C) mixed  $\mu$ E containing **L5**, (D) single  $\mu$ E containing **L2**, (E) mixed  $\mu$ E containing **L2**, (F) single  $\mu$ E containing **L3**, (G) mixed  $\mu$ E containing **L3**.

### Enhanced activity of the NHC-precursor in the confined environment of w/o microemulsion

We chose 4-iodotoluene (1.0 equiv.) and *n*-butyl acrylate (1.2 equiv.) as coupling partners of our model system in the presence of triethylamine (2.0 equiv.) to investigate the catalytic performance of imidazo[1,5- $\alpha$ ]pyridinium salt **L1** as a ligand in the palladium catalysed Mizoroki–Heck reaction in w/o microemulsion

(2.0 mL). All three types of microemulsion (anionic, nonionic and mixed) systems were screened to obtain the most suitable reaction medium. The Heck reaction was performed with *in situ* generated 2 mol% Pd–NHC (1:2) complex. The reaction progressed smoothly to completion within 45 min. at 50 °C, resulting in the desired cross-coupled product ((*E*)-<sup>u</sup>butyl-3-(*p*-tolyl)acrylate) **5a** along with the homo-coupled product (Table 1, entries 1–3). In anionic (SDS), mixed (SDS and Brij-35) and non-ionic (Brij-35) microemulsion systems, 46%, 55% and 40% of the desired Heck coupled product (entries 1–3) were obtained, respectively. The reaction was also performed in the absence of an additive or in water or IPM as solvent to validate the superior activity of the NHC-precursor in the confined environment (entries 4–8). All these results are summarized in Fig. 2 (bar diagram) and Table 1. The formation of cross-coupled product was confirmed by spectral analysis.<sup>22</sup> Further optimization with water soluble bases, *e.g.* potassium carbonate and tetramethyl ethylenediamine (TMEDA), produced almost comparable yields of the desired product, 43% and 46%, respectively (entries 9 and 10), whereas for triethylamine (TEA), 55% of the Heck product was obtained (entry 2). It is noteworthy that stoichiometric amount of base was essential for the reaction, to neutralize the acid produced (herein, HI) in the reaction medium. Moreover, the higher yield of the Heck reaction in mixed microemulsion systems suggests predominant ion–dipole interactions between mixed surfactant polar head group and TEA within a confined environment.

**Table 1** Screening of reaction conditions for the C–C cross-coupling Heck reaction<sup>a</sup>

Entry	Solvent	NHC-precursor (L)	Base	5 <sup>b</sup> (%)
1	Anionic surfactant (SDS) blended (w/o) $\mu$ E	<b>L1</b>	Et <sub>3</sub> N	46
2	Mixed surfactant (SDS/Brij-35) blended (w/o) $\mu$ E	<b>L1</b>	Et <sub>3</sub> N	55
3	Non-ionic surfactant (Brij-35) blended (w/o) $\mu$ E	<b>L1</b>	Et <sub>3</sub> N	40
4	Water <sup>c</sup>	—	Et <sub>3</sub> N	Trace (7) <sup>d</sup>
5	Isopropyl myristate (IPM) <sup>c</sup>	—	Et <sub>3</sub> N	8 (11) <sup>d</sup>
6	Anionic surfactant (SDS) blended (w/o) $\mu$ E	—	Et <sub>3</sub> N	30 (35) <sup>d</sup>
7	Mixed surfactant (SDS/Brij-35) blended (w/o) $\mu$ E	—	Et <sub>3</sub> N	38 (41) <sup>d</sup>
8	Non-ionic surfactant (Brij-35) blended (w/o) $\mu$ E	—	Et <sub>3</sub> N	31 (35) <sup>d</sup>
9	Mixed surfactant (SDS/Brij-35) blended (w/o) $\mu$ E	<b>L1</b>	K <sub>2</sub> CO <sub>3</sub>	43
10	Mixed surfactant (SDS/Brij-35) blended (w/o) $\mu$ E	<b>L1</b>	TMEDA	46
11	Anionic surfactant (SDS) blended (w/o) $\mu$ E	<b>L2</b>	Et <sub>3</sub> N	65
12	Mixed surfactant (SDS/Brij-35) blended (w/o) $\mu$ E	<b>L2</b>	Et <sub>3</sub> N	82 (88) <sup>d</sup>
13	Non-ionic surfactant (Brij-35) blended (w/o) $\mu$ E	<b>L2</b>	Et <sub>3</sub> N	49
14	Anionic surfactant (SDS) blended (w/o) $\mu$ E	<b>L3</b>	Et <sub>3</sub> N	50
15	Mixed surfactant (SDS/Brij-35) blended (w/o) $\mu$ E	<b>L3</b>	Et <sub>3</sub> N	62
16	Non-ionic surfactant (Brij-35) blended (w/o) $\mu$ E	<b>L3</b>	Et <sub>3</sub> N	44
17	Anionic surfactant (SDS) blended (w/o) $\mu$ E	<b>L4</b>	Et <sub>3</sub> N	52
18	Mixed surfactant (SDS/Brij-35) blended (w/o) $\mu$ E	<b>L4</b>	Et <sub>3</sub> N	66
19	Non-ionic surfactant (Brij-35) blended (w/o) $\mu$ E	<b>L4</b>	Et <sub>3</sub> N	45
20	Anionic surfactant (SDS) blended (w/o) $\mu$ E	<b>L5</b>	Et <sub>3</sub> N	56
21	Mixed surfactant (SDS/Brij-35) blended (w/o) $\mu$ E	<b>L5</b>	Et <sub>3</sub> N	73
22	Non-ionic surfactant (Brij-35) blended (w/o) $\mu$ E	<b>L5</b>	Et <sub>3</sub> N	47

<sup>a</sup> Unless otherwise mentioned, reactions were performed at 50 °C for 45 min using aryl halides (0.5 mmol), <sup>u</sup>butyl acrylate (0.6 mmol), base (1 mmol), Pd(OAc)<sub>2</sub> (2 mol%), **L** (4 mol%), in 2 mL of microemulsion containing 0.5 mmol of surfactant with  $\omega = 20$ . <sup>b</sup> Isolated yields. <sup>c</sup> Reaction was performed in 2 mL of corresponding pure solvent. <sup>d</sup> HPLC yield.

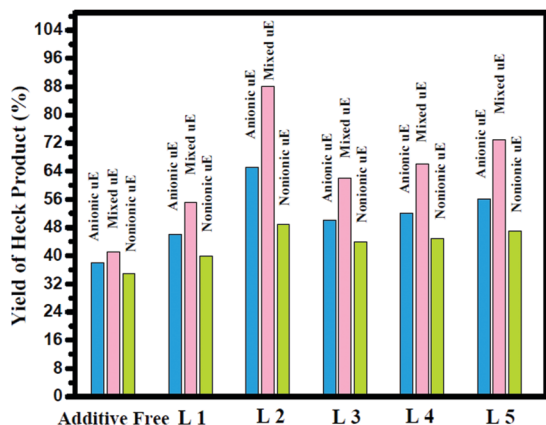
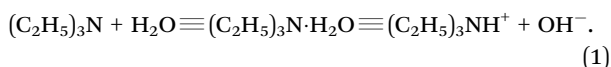


Fig. 2 The Mizoroki–Heck reaction between 4-iodotoluene and *n*-butyl acrylate in the presence of imidazolium salts (L1–L5) as additive.

This increases the availability of TEA in the vicinity of the interfacial region and in confined water. Consequently, the formation of OH<sup>−</sup> base surrounding the interface is expected to proceed in the following way:<sup>24</sup>



Here, penetration of OH<sup>−</sup> in the palisade layer of w/o microemulsion cannot be ruled out, and subsequently, a basic environment in the vicinity of the interface appears to be advantageous for the catalytic efficiency. The inherent problem of using IPM based biocompatible microemulsion as organic reaction media is associated with the high boiling nature of IPM which makes the isolation procedure a little cumbersome and tends to limit its application. We have developed a novel separation method where IPM is converted to myristic acid with the application of dilute acid under mild conditions and precipitated out from the reaction medium. Thereafter, a regular workup followed by a purification allows easy recovery of the desired product.<sup>22</sup>

#### Evaluation of reactivity of NHC-carbene precursors (L2–L5) in w/o microemulsion for the Mizoroki–Heck reaction

Encouraged by the findings, catalytic efficiency of a series of NHC-precursors (L2–L5) was screened in our model system for the Pd-catalyzed Heck reaction at  $\omega$  20 following the procedure discussed in the previous section. In all these cases, the reaction proceeded smoothly to completion and all the data are presented in Table 1 (entries 11–22). Interestingly, the highest yield of the Heck product was obtained in the mixed microemulsion system using L2 (yield 88%, Table 1, entry 12). With other precursors L3, L4 and L5, 62%, 66% and 73% yields were obtained, respectively (entries 15, 18 and 21). Further, dependence of the catalytic activity on the micro-heterogeneity of the microemulsion was studied by varying various components like water content ( $\omega$ ), additive and palladium concentration. Upon increasing water content of the microemulsion ( $\omega$  from 20 to 50), the yield of the desired product dropped from 88% to 48% (Table 2, entries 1–4) probably due to a decrease in ion–dipole

Table 2 Optimization of the Heck reaction<sup>a</sup>

Entry	Solvent <sup>b</sup>	Catalyst (x mol%)	L2 (y mol%)	Yield <sup>c</sup> (%)
1.	w/o mixed $\mu\text{E}$ , $\omega = 20$	Pd(OAc) <sub>2</sub> (2 mol%)	4	88 <sup>d</sup>
2.	w/o mixed $\mu\text{E}$ , $\omega = 30$	Pd(OAc) <sub>2</sub> (2 mol%)	4	71
3.	w/o mixed $\mu\text{E}$ , $\omega = 40$	Pd(OAc) <sub>2</sub> (2 mol%)	4	61
4.	w/o mixed $\mu\text{E}$ , $\omega = 50$	Pd(OAc) <sub>2</sub> (2 mol%)	4	48
5.	w/o mixed $\mu\text{E}$ , $\omega = 20$	Pd(OAc) <sub>2</sub> (4 mol%)	4	89
6.	w/o mixed $\mu\text{E}$ , $\omega = 20$	Pd(OAc) <sub>2</sub> (1 mol%)	4	69
7.	w/o mixed $\mu\text{E}$ , $\omega = 20$	PdCl <sub>2</sub> (2 mol%)	4	76
8.	w/o mixed $\mu\text{E}$ , $\omega = 20$	Pd(OAc) <sub>2</sub> (2 mol%)	2	71
9.	w/o mixed $\mu\text{E}$ , $\omega = 20$	Pd(OAc) <sub>2</sub> (2 mol%)	6	60
10. <sup>e</sup>	DMF, 90 °C	Pd(OAc) <sub>2</sub> (2 mol%)	4	85
11. <sup>e</sup>	DMF : H <sub>2</sub> O (9 : 1), 90 °C	Pd(OAc) <sub>2</sub> (2 mol%)	4	62

<sup>a</sup> Reactions were performed at 50 °C for 45 minutes using 4-iodotoluene (0.5 mmol), *n*-butyl acrylate (0.6 mmol), triethylamine (1 mmol), in 2 mL of solvent. <sup>b</sup> Reactions were performed in mixed surfactant (SDS/Brij-35) blended (w/o) microemulsion as solvent unless otherwise mentioned. <sup>c</sup> Isolated yields. <sup>d</sup> HPLC yield. <sup>e</sup> Reaction was continued overnight.

interactions between the surfactant head group and TEA which resulted from a decrease in surfactant concentration on the droplet surface. These results suggest that the reaction took place neither in the water nor in the oil domain exclusively; rather, it occurred in the palisade layer of the oil–water interface of the microemulsion. The inference is well corroborated by previous reports where the most plausible reaction location was identified to be either interfacial region or within the surfactant palisade layer of the w/o microemulsion.<sup>12,14a,25</sup>

The methodology was further optimized by altering the metal salt (Pd(II) acetate, Pd(II) chloride, *etc.*), mol% ligand, *etc.* The experimental findings are summarized in Table 2. A nearly equal yield of the Heck product was obtained by loading 2 or 4 mol% Pd(II) acetate (Table 2, entries 1 and 5). However, considering the development of greener protocol, further studies are conducted with 2 mol% *in situ* generated Pd–NHC complex (1 : 2) using L2 in mixed  $\mu\text{E}$  system. Any deviation from these optimized condition produced a lower yield of the Heck product (Table 2, entries 8 and 9) which demonstrated a crucial role of the ligand and system composition in the Heck reaction. Nevertheless, the reaction proceeded in common organic solvents *viz.* DMF and DMF–water mixture yielding 85% and 62% desired product, respectively, only after overnight heating at 90 °C (entries 10 and 11). These results signify the improved performance of the Mizoroki–Heck reaction in the microemulsion in contrast to commonly used organic solvents.

In order to investigate the substrate scope of the methodology, a number of aryl halides, *e.g.* activated and non-activated aryl iodides, bromides and chlorides, were treated with *n*-butyl acrylate under optimized condition. The reaction proceeded efficiently with a range of electron deficient and electron rich aryl iodides, and non-activated aryl bromides (Table 3, entries 1–7). With activated and

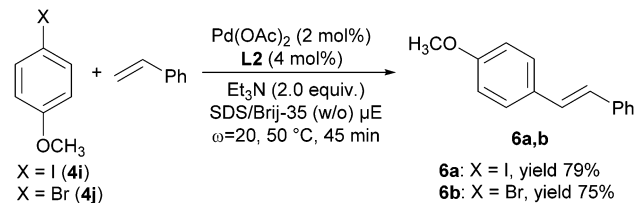
**Table 3** Mizoroki–Heck reaction with aryl halides and <sup>n</sup>butylacrylate in ligand (L2) encapsulated w/o mixed microemulsion<sup>a</sup>

Entry	Aryl halide (4)	5, yield <sup>b</sup>
	X = I, Br, Cl	
1		<b>5a, 88%<sup>c</sup></b>
2		<b>5b, 84%</b>
3		<b>5c, 68%</b>
4		<b>5d, 85%</b>
5		<b>5e, 64%</b>
6		<b>5a, 74%</b>
7		<b>5a, 17%</b>
8		<b>5f, 33%</b>

<sup>a</sup> Reactions were performed at 50 °C for 45 minutes using aryl halide (1.0 equiv.), <sup>n</sup>butyl acrylate (1.2 equiv.), triethylamine (2 equiv.), Pd(OAc)<sub>2</sub> (2 mol%), L2 (4 mol%) in mixed surfactant (SDS/Brij-35) blended (w/o) microemulsion as solvent at  $\omega$  20. <sup>b</sup> Isolated yields of the products. <sup>c</sup> HPLC yield.

non-activated aryl chlorides, the Heck product yield was only 17% and 33%, respectively (Table 3, entries 7 and 8).

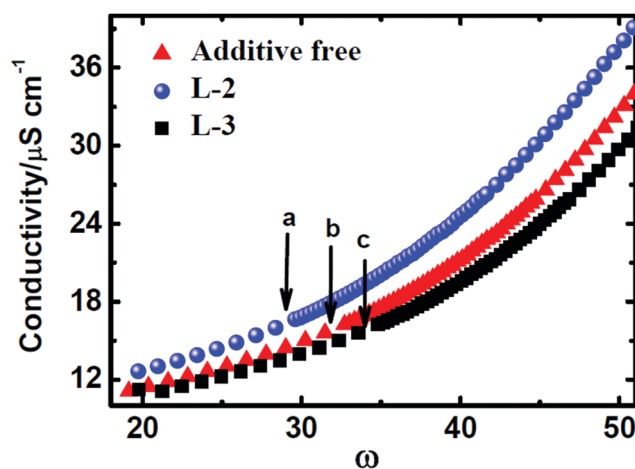
To broaden the substrate scope further, the coupling partner was changed from acrylate to styrene (Scheme 2). To our delight, the cross-coupling reaction proceeded smoothly to afford asymmetrical stilbene derivative (6) with both electron rich aryl iodide and bromide in high yields (79% and 75%, respectively).

**Scheme 2** The Mizoroki–Heck reaction of aryl halides with styrene within Pd–NHC encapsulated w/o mixed microemulsion.

### Enhanced flexibility of the NHC-precursor encapsulated droplet nanoreactor

To further examine any correlation between the observed rate enhancement in the Heck reaction and the active NHC-precursor L2 (as ligand), conductivity measurements were carried out in mixed  $\mu$ E system (water/SDS/Brij-35/Pn/IPM). The change in conductivity of the system was measured by varying the water content ( $\omega$ ) of the medium in the presence of the active NHC-precursor (L2) at 50 °C. The conductance data are plotted as a function of  $\omega$  (Fig. 3). Initially, conductivity increased gradually up to  $\omega \sim 30$ ; thereafter, a steeper increase in the overall conductivity of the system was observed (L2, Fig. 3). Control experiments without NHC-precursors were also performed for comparison. The critical value for a sharp linear increase in conductivity is known as percolation threshold point.<sup>26</sup> As per the general idea, if droplets are non-interacting hard sphere type, no significant increase in conductance occurs, whereas, with an increase in fluidity of the droplet interface, a sharp rise in conductance is expected as a result of faster coalescence of water droplets. This fission and fusion process permits fast material exchange which essentially promotes the rates of organic reactions.<sup>13b,27</sup>

The influence of the ligand structure (L2) was monitored by control experiments where conductivity of the system was measured (i) without ligand and (ii) with ligand L3 in which free OH functionality of imidazopyridine salt L2 is substituted with (–OMe) group (Scheme 1). The conductivity vs.  $\omega$  plot

**Fig. 3** Electrical conductivity of SDS/Brij-35 blended w/o mixed surfactant microemulsion in the absence and presence of an active NHC-precursor.

(curves a–c, Fig. 3) displayed similar patterns in all the three cases. The maximum increase in the conductivity was noted for  $\mu\text{E}$  system containing L2 with a simultaneous increase in percolation threshold point in comparison to ligand free or L3 encapsulated  $\mu\text{E}$  system. A significant increase in percolation in L2 containing  $\mu\text{E}$  indicates a better attractive interaction among the droplets which possibly allows material exchange at a faster rate.<sup>28</sup> This phenomenon advocates for a higher efficiency of the Mizoroki–Heck reaction within the nano-reactor. The relatively low yields of the Heck product in precursor free or L3 containing  $\mu\text{E}$  systems also corroborates the above fact (Table 1, entry 15). It can be noted that free OH functionality of L2 can make hydrogen bond with surfactant charged head group present at the interface, changing the interfacial architecture of nano-reactor within the confinement. Similar studies correlating the effect of additives on changing interfacial flexibility *vis-à-vis* percolation threshold of microemulsion systems by conductivity experiments have previously been reported.<sup>25a</sup>

### Extended H-bonding network in the presence of the NHC-precursor in the confinement

Possible alteration of water microstructure within the confinement was monitored employing FTIR measurement *via*  $\text{D}_2\text{O}$  probing. The study was conducted with the imidazolium salt (L2) encapsulated mixed microemulsion system at a fixed water content ( $\omega = 20$ ) at  $30^\circ\text{C}$ . The sample was prepared using 10%  $\text{D}_2\text{O}$  containing water which forms HOD through rapid exchange between H and D atoms.<sup>18b</sup> Use of HOD as a probe is particularly advantageous as the O–D band can be decoupled from the O–H band appearing in a region of  $2200\text{ cm}^{-1}$  to  $2700\text{ cm}^{-1}$ . This region corresponds to the fingerprint region of the vibrational stretch of O–D bonds in water<sup>29</sup> which remain comparatively separated from other strong absorption bands of the constituents of the microemulsion and/or the additive.<sup>19b</sup> Earlier reports showed water molecules exist in three ‘states’ or ‘layers’ in w/o microemulsion which are detectable through FTIR measurements.<sup>30</sup> The corresponding O–D bands are fitted as the sum of Gaussian bands using Gaussian curve fitting program following a three-state model which confirms the existence of water molecules in three different modes inside the nano-pool, namely (i) free water, (ii) bound water and (iii) trapped water. The deconvoluted FTIR spectra (experimental) are depicted in Fig. 4A and B. According to this model, free water

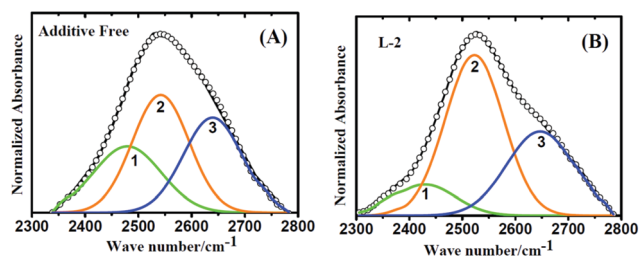


Fig. 4 FTIR study of SDS/Brij-35 blended w/o mixed surfactant microemulsion (A) in the absence and (B) in the presence of an active NHC-precursor (10%  $\text{D}_2\text{O}$ ).

molecules occupy the cores of the water pool of w/o microemulsion and possess a strong hydrogen bonding network among themselves, *i.e.* their properties are similar to bulk water. Such a H-bond shifts the O–D stretching band towards lower frequency region around  $2450\text{ cm}^{-1}$ . The bound water, *viz.* the surfactant head group-bound water molecules, appear around  $2550\text{ cm}^{-1}$ . The water molecules dispersing within long hydrocarbon chains of the surfactant are termed ‘trapped water’ which is matrix-isolated dimeric or monomeric in nature and absorbs around  $2650\text{ cm}^{-1}$ .

A comparison between the individual curves 1–3 of Fig. 4A vs. B demonstrates that the presence of the NHC-precursor L2 in water pool of microemulsion causes substantial perturbation of water microstructures in which the abundance of free water was decreased (curve 1), the population of bound water was increased (curve 2) and the population of trapped water exhibited a marginal variation (curve 3). The bound water molecules generally reside at the interfacial region. The increase in bound water content in the presence of L2 suggested that L2 essentially resided at the interface. This allowed a change in the hydrogen bonding network dynamics of water within the nano-confinement which was correlated with the rate enhancement of the Heck reaction.

### Role of palladium

*In situ* formation of Pd–NHC complex is strongly suggested from the  $^{13}\text{C}$  NMR spectrum of freshly prepared Pd–NHC in encapsulated microemulsion system, accorded in  $\text{D}_2\text{O}$ . The characteristic C2 signal of free NHC species L2 was found to shift from 149.6 ppm to 175 ppm (Fig. 5). A downfield shift of the same carbon ( $\sim 20\text{ ppm}$ ) for Pd–NHC complex is consistent with the data reported earlier.<sup>7a,b,31</sup> In the  $^{13}\text{C}$  NMR spectrum recorded after the product recovery, from the aqueous layer containing Pd–NP, the Pd–NHC peak at 175 ppm still persisted, albeit in a low intensity. We believe that the probable accumulation of the NHC-precursor L2 containing OH functionality at the interface influences the availability of *in situ* generated Pd–NHC in the vicinity of the reaction site, which facilitated the Mizoroki–Heck reaction.

In the HRTEM measurement after the nanoparticle formation, we observed Pd–NP of average size  $5.53 \pm 0.63\text{ nm}$  forming an assembly of nanoparticles with an average size of  $\sim 25\text{ nm}$  (Fig. 6).<sup>7c,32</sup> It is likely that the Pd–NPs owe their stability during repetitive catalytic cycles to such a cluster formation. The catalyst was recycled up to four times. After the second cycle 77% of the product was isolated. Similarly, the third and fourth cycles afforded the desired product in 69% and 58% yields, respectively. A significant decrease in the yield of the Mizoroki–Heck reaction

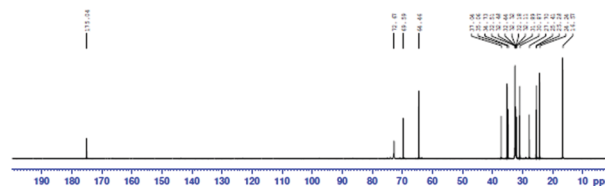


Fig. 5  $^{13}\text{C}$  NMR spectrum showing the formation of a Pd–NHC species.

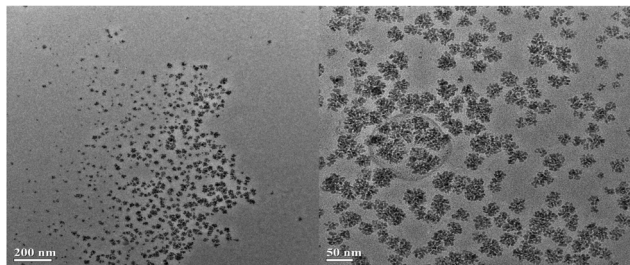


Fig. 6 High resolution transmission electron microscopy (HRTEM) analysis of isolated Pd nano-cluster in w/o mixed microemulsion (SDS/Brij-35/Pn/IPM) in the presence of additive L2 (at two different magnifications).

was observed after the fourth cycle, possibly because of the agglomeration of Pd(0) particles.

## Experimental procedure

### General procedure of the Heck reaction

Into a 10 mL glass reaction vial fitted with screw cap, 2 mL microemulsion (water/SDS/Brij-35/Pn/IPM) of fixed  $\omega$  ( $=$  [water]/[surfactant]), 4 mol% active NHC-precursor (L) (0.02 mmol) and 2 mol% Pd(OAc)<sub>2</sub> (0.01 mmol) were added. The mixture was placed in a preheated oil bath at 30 °C with constant sonication till all the solid material dissolved. Into this mixture were added 4-iodotoluene (0.5 mmol), *n*-butyl acrylate (0.6 mmol) and triethylamine (1.0 mmol), and the mixture was heated at 50 °C for 45 min. The progress of the reaction was monitored by thin layer chromatography (TLC) on silica gel.

### Workup procedure to break IPM based biocompatible microemulsion

After the appropriate time, the reaction vessel was charged with 15 mg solid NaCl followed by 3 mL of 0.6 N HCl. The mixture was stirred for 30 min till an off-white precipitate of myristic acid appeared. An additional 10 min stirring was continued for the complete precipitation of insoluble materials. The mixture was filtered and the filtrate was extracted with ethyl acetate (3 × 10 mL). The collected organic layer was washed with brine, dried over anhydrous sodium sulphate and the solvent was removed under reduced pressure. The residue was purified by column chromatography on silica gel using a mixture of ethyl acetate and petroleum ether (1 : 99).

The formation of the desired products was confirmed through <sup>1</sup>H NMR and <sup>13</sup>C NMR.<sup>22</sup> Similar concentration ratio of reagents was maintained, in the case of experiments conducted in other solvents.

### Procedure for recycling

The reaction was performed in 2.5 mmol scale following the above procedure. After the first run, excess IPM (~ 15 mL) was added and the mixture was sonicated. A biphasic system was formed from which the supernatant organic layer was taken out with the help of a micropipette. Into the aqueous layer containing Pd–NHC nanocluster were added necessary amounts of Brij-35,

IPM which was sonicated to result in fresh microemulsion formulation. Fresh starting materials, IPM (oil), Pn (co-surfactant) and nonionic surfactant (Brij-35) were added (as these components could be removed at the time of product extraction) to the remnant aqueous part which contained the catalytic system and anionic surfactant (SDS) from the first run.

## Conclusion

We have successfully developed an operationally simple protocol for the Mizoroki–Heck reaction with high yields under relatively mild conditions. Novel (1,5- $\alpha$ )-imidazo-pyridinium chlorides were synthesized as NHC-precursors in w/o microemulsion (water/SDS/Brij-35/Pn/IPM) as an unconventional solvent system. NMR evidence for the formation of Pd–NHC molecular complex suggests catalysis by a Pd–NHC complex in the confinement of an organized nanoreactor accompanied by an enhanced rate of reaction. It is possible that the phenolic –OH group of the ligand L2 allows its accumulation at the aqueous interface localizing the catalyst concentration. The formation of microassembly of nanoparticles (Pd nanocluster) is indicative of the reservoir of Pd during catalysis. The applications of the present w/o microemulsion system in similar organic transformations, and their further mechanistic elucidation are currently under study in our laboratory.

## Conflicts of interest

There are no conflicts to declare.

## Acknowledgements

K. G. thanks SERB, DST, India (grant number SB/FT/CS-032/2012), CSIR, India (grant number 02(0326)/17/EMR-II) and Presidency University (FRPDF grant) for financial support. We thank Presidency University and IIT Kanpur for instrumental supports. S. D. thanks SERB, DST, India, for research fellowship.

## Notes and references

- Some selected references: (a) A. J. Arduengo, *Acc. Chem. Res.*, 1999, **32**, 913–921; (b) W. A. Herrmann, *Angew. Chem., Int. Ed.*, 2002, **41**, 1290–1309; (c) F. E. Hahn and M. C. Jahnke, *Angew. Chem., Int. Ed.*, 2008, **47**, 3122–3172; (d) S. D. Gonzalez, N. Marion and S. P. Nolan, *Chem. Rev.*, 2009, **109**, 3612–3676; (e) H. Jacobsen, A. Correa, A. Poater, C. Costabile and L. Cavallo, *Coord. Chem. Rev.*, 2009, **253**, 687–703; (f) D.-C. Thomas Dröge and F. Glorius, *Angew. Chem., Int. Ed.*, 2010, **49**, 6940–6952; (g) C. M. Latham, W. Lewis, A. J. Blake and S. Woodward, *Eur. J. Org. Chem.*, 2015, 1819–1823.
- Some selected references: (a) E. Peris and R. H. Crabtree, *Coord. Chem. Rev.*, 2004, **248**, 2239; (b) N. Marion, O. Navarro, J. Mei, E. D. Stevens, N. M. Scott and S. P. Nolan, *J. Am. Chem. Soc.*, 2006, **128**, 4101–4111; (c) L. H. Gade and S. Bellemin-Lapognaz, *Coord. Chem. Rev.*, 2007, **251**, 718; (d) E. A. B. Kantchev,

- C. J. O. Brien and M. G. Organ, *Angew. Chem., Int. Ed.*, 2007, **46**, 2768–2813; (e) X.-F. Wu, P. Anbarasan, H. Neumann and M. Beller, *Angew. Chem., Int. Ed.*, 2010, **49**, 9047–9050; (f) G. C. Fortman and S. P. Nolan, *Chem. Soc. Rev.*, 2011, **40**, 5151–5169; (g) S. Würtz and F. Glorius, *Acc. Chem. Res.*, 2008, **41**, 1523–1533; (h) C. Valente, S. Calimsiz, K. H. Hoi, D. Mallik, M. Sayah and M. G. Organ, *Angew. Chem., Int. Ed.*, 2012, **51**, 3314–3332; (i) H. Li, C. C. C. Johansson Seechurn and T. J. Colacot, *ACS Catal.*, 2012, **2**, 1147–1164; (j) P. G. Gildner and T. J. Colacot, *Organometallics*, 2015, **34**, 5497–5508.
- 3 (a) L. Oehninger, R. Rubbiani and I. Ott, *Dalton Trans.*, 2013, **42**, 3269–3284; (b) F. Hackenberg, H. Müller-Bunz, R. Smith, W. Streciwilk, X. Zhu and M. Tacke, *Organometallics*, 2013, **32**, 5551–5560; (c) K. M. Hindi, M. J. Panzner, C. A. Tessier, C. L. Cannon and W. J. Youngs, *Chem. Rev.*, 2009, **109**, 3859–3884; (d) F. Lazreg and C. S. J. Cazin, *Medical Applications of NHC-Gold and -Copper Complexes*, in *N-Heterocyclic Carbenes: Effective Tools for Organometallic Synthesis*, ed. S. P. Nolan, Wiley-VCH Verlag GmbH & Co. KGaA, 2014, ch. 7, pp. 173–198.
- 4 (a) C. I. Ezugwu, N. A. Kabir, M. Yusubov and F. Verpoort, *Coord. Chem. Rev.*, 2016, **307**, 188–210; (b) A. B. Miguel-Coello, M. Bardaji, S. Coco, B. Donnio, B. Heinrich and P. Espinet, *Inorg. Chem.*, 2018, **57**, 4359–4369; (c) X. Zhang, B. Cao, E. J. Valente and T. K. Hollis, *Organometallics*, 2013, **32**, 752–761.
- 5 A. V. Astakhov, O. V. Khazipov, A. Y. Chernenko, D. V. Pasyukov, A. S. Kashin, E. G. Gordeev, V. N. Khrustalev, V. M. Chernyshev and V. P. Ananikov, *Organometallics*, 2017, **36**, 1981–1992.
- 6 (a) S. Chandrasekhar, C. Narsihmulu, S. S. Sultana and N. R. Reddy, *Org. Lett.*, 2002, **4**, 4399–4401; (b) T. Dwars, E. Paetzold and G. Oehme, *Angew. Chem., Int. Ed.*, 2005, **44**, 7174–7199; (c) L. Yu, Y. Huang, Z. Wei, Y. Ding, C. Su and Q. Xu, *J. Org. Chem.*, 2015, **80**, 8677–8683; (d) T. Kitanosono, K. Masuda, P. Xu and S. Kobayashi, *Chem. Rev.*, 2018, **118**, 679–746; (e) J. Chen, J. Wu and T. Tu, *ACS Sustainable Chem. Eng.*, 2017, **5**, 11744–11751.
- 7 (a) G. Zhang, H. Zhou, J. Hu, M. Liu and Y. Kuang, *Green Chem.*, 2009, **11**, 1428–1432; (b) M. Hejazifar, M. Earle, K. R. Seddon, S. Weber, R. Zirbs and K. Bica, *J. Org. Chem.*, 2016, **81**, 12332–12339; (c) M. Taskin, A. Cognigni, R. Zirbs, E. Reimhult and K. Bica, *RSC Adv.*, 2017, **7**, 41144–41151; (d) P. Migowski and J. Dupont, *Chem. – Eur. J.*, 2007, **13**, 32–39; (e) J. Dupont, *Acc. Chem. Res.*, 2011, **44**, 1223–1231.
- 8 H.-J. Xu, Y.-Q. Zhao and X.-F. Zhou, *J. Org. Chem.*, 2011, **76**, 8036–8041.
- 9 B. H. Lipshutz and B. R. Taft, *Org. Lett.*, 2008, **10**, 1329–1332.
- 10 (a) V. Calo, A. Nacci, L. Lopez and N. Mannarini, *Tetrahedron Lett.*, 2000, **41**, 8973–8976; (b) J.-Z. Jiang and C. Cai, *J. Colloid Interface Sci.*, 2006, **299**, 938–943.
- 11 K. Holmberg, *Eur. J. Org. Chem.*, 2007, 731–742 & references therein.
- 12 (a) I. Danielsson and B. Lindman, *Colloids Surf.*, 1981, **3**, 391–392; (b) S. Bardhan, K. Kundu, G. Chakraborty, S. K. Saha and B. K. Paul, *J. Surfactants Deterg.*, 2015, **18**, 547–567.
- 13 (a) M. Häger, F. Currie and K. Holmberg, *Organic Reactions in Microemulsions*, in *Colloid Chemistry II. Topics in Current Chemistry*, ed. M. Antonietti, Springer, Berlin, Heidelberg, 2003, vol. 227, pp. 53–74; (b) M. A. Lpez-Quintelaa, C. Tojob, M. C. Blancoa, L. GarcíaRioa and J. R. Leis, *Curr. Opin. Colloid Interface Sci.*, 2004, **9**, 264–278.
- 14 (a) J. Eastoe, M. J. Hollamby and L. Hudson, *Adv. Colloid Interface Sci.*, 2006, **5**, 128–130; (b) A. K. Ganguli and S. Vaidya, *Chem. Soc. Rev.*, 2010, **39**, 474–485.
- 15 S. P. Moulik and B. K. Paul, *Adv. Colloid Interface Sci.*, 1998, **78**, 99–195.
- 16 (a) J. G. de Vries, *Dalton Trans.*, 2006, 421–429; (b) F. Christoffel and T. R. Ward, *Catal. Lett.*, 2018, **148**, 489–511.
- 17 (a) I. Volovych, Y. Kasaka, M. Schwarze, Z. Nairoukh, J. Blum, M. Fanun, D. Avnir and R. Schomäcker, *J. Mol. Catal. A: Chem.*, 2014, **393**, 210–221; (b) A.-E. Wang, J.-H. Xie, L.-X. Wang and Q.-L. Zhou, *Tetrahedron*, 2005, **61**, 259–266; (c) S. Bhattacharya, A. Srivastava and S. Sengupta, *Tetrahedron Lett.*, 2005, **46**, 3557–3560.
- 18 (a) S. Bardhan, K. Kundu, S. K. Saha and B. K. Paul, *J. Colloid Interface Sci.*, 2013, **411**, 152–161; (b) *Colloids in Biotechnology*, ed. M. Fanun, CRC Press, USA, 2011; (c) S. Bardhan, K. Kundu, G. Chakraborty, B. K. Paul, S. P. Moulik and S. K. Saha, *Bio-inspired microemulsions and their strategic pharmacological perspectives*, in *Encyclopedia of Biocolloid and Biointerface Science*, ed. H. Ohshima, John Wiley & Sons, New Jersey, USA, 2016, ch. 10, pp. 122–144.
- 19 (a) F. Lopez, G. Cinelli, L. Ambrosone, G. Colafemmina, A. Ceglie and G. Palazzo, *Colloids Surf., A*, 2004, **49**, 237–243; (b) M. L. Curri, A. Agostino, L. Manna, M. D. Monica, M. Catalano, L. Chiavarone, V. Spagnolo and M. Lugara, *J. Phys. Chem. B*, 2000, **104**, 8391–8397.
- 20 (a) *Mixed Surfactant Systems*, ed. J. F. Scamehorn, K. Ogino and M. Abe, Dekker, New York, 1993; (b) S. Bardhan, K. Kundu, S. Das, M. Poddar, S. K. Saha and B. K. Paul, *J. Colloid Interface Sci.*, 2014, **430**, 129–139; (c) S. Bardhan, K. Kundu, B. Kar, G. Chakraborty, D. Ghosh, D. Sarkar, S. Das, S. Senapati, S. K. Saha and B. K. Paul, *RSC Adv.*, 2016, **6**, 55104–55116; (d) E. Odella, R. D. Falcone, J. J. Silber and N. M. Correa, *J. Phys. Chem. B*, 2018, **122**, 4366–4375.
- 21 J. T. Hutt and Z. D. Aron, *Org. Lett.*, 2011, **13**, 5256–5259.
- 22 See ESI†.
- 23  $\omega$  denote mole ratio of water vs. surfactant.
- 24 N. Li, Q. Cao, Y. Gao, J. Zhang, L. Zheng, X. Bai, B. Dong, Z. Li, M. Zhao and L. Yu, *Chem. Phys. Chem.*, 2007, **8**, 2211–2217.
- 25 (a) A. Cid, J. F. Galvez, E. Barreiro and J. C. Mejuto, *Tenside, Surfactants, Deterg.*, 2018, **55**, 110–115; (b) S. K. Mehta, K. Kaur, E. Arora and K. K. Bhasin, *J. Phys. Chem. B*, 2009, **113**, 10686–10692; (c) M. Hager, U. Olsson and K. Holmberg, *Langmuir*, 2004, **20**, 6107–6115; (d) K. Holmberg, *Curr. Opin. Colloid Interface Sci.*, 2003, **8**, 187–196; (e) J. Sjöblom, R. Lindberg and S. E. Friberg, *Adv. Colloid Interface Sci.*, 1996, **65**, 125–287; (f) M.-J. Schwuger, K. Stickdorn and R. Schomaecker, *Chem. Rev.*, 1995, **95**, 849–864.

- 26 X. Zhang, Y. Chen, J. Liu, C. Zhao and H. Zhang, *J. Phys. Chem. B*, 2012, **116**, 3723–3734.
- 27 A. Jada, J. Lang and R. Zana, *J. Phys. Chem.*, 1989, **93**, 10–12.
- 28 P. D. I. Fletcher, A. M. Howe and B. H. Robinson, *J. Chem. Soc., Faraday Trans. 1*, 1987, **83**, 985–1006.
- 29 E. E. Fenn, D. B. Wong and M. D. Fayer, *Proc. Natl. Acad. Sci. U. S. A.*, 2009, **106**, 15243–15248.
- 30 (a) T. K. Jain, M. Varshney and A. Maitra, *J. Phys. Chem.*, 1989, **93**, 7409; (b) Y. Gao, N. Li, L. Zheng, X. Bai, L. Yu, X. Zhao, J. Zhang, M. Zhao and Z. Li, *J. Phys. Chem. B*, 2007, **111**, 2506–2513.
- 31 (a) H. Lebel, M. K. Janes, A. B. Charette and S. P. Nolan, *J. Am. Chem. Soc.*, 2004, **126**, 5046–5047; (b) C. Burstein, C. W. Lehmann and F. Glorius, *Tetrahedron*, 2005, **61**, 6207–6217.
- 32 An enlarged view of Fig. 6 (Fig S2) is included in ESI†.